Thermochimica Acta 494 (2009) 40–44

Contents lists available at ScienceDirect

Thermochimica Acta

journal homepage: www.elsevier.com/locate/tca

Thermophysical properties of Ni80Cr20

T. Hüpf[a,*], C. Cagran[a], E. Kaschnitz[b], G. Pottlacher[a]

[a] Institut für Experimentalphysik, Technische Universität Graz, Petersgasse 16, 8010 Graz, Austria
[b] Österreichisches Gießerei-Institut, Parkstraße 21, 8700 Leoben, Austria

ARTICLE INFO

Article history:
Received 12 March 2009
Received in revised form 15 April 2009
Accepted 17 April 2009
Available online 24 April 2009

Keywords:
Alloys
Inconel 718
Liquid metals
Nickel
Ni80Cr20
Pulse-heating
Resistivity

ABSTRACT

The fast pulse-heating method provides a possibility to investigate thermophysical properties in the liquid state of electrically conducting materials in terms of a containerless measurement technique. Thereby wire-shaped specimens are rapidly heated by the passage of a large current pulse. This leads to heating rates of 10^8 K/s and an experimental duration of typically 50 μs. In addition to pure elements, multi-component alloys of industrial relevance and more simple alloys like Ni80Cr20 are in our focus of interest. Measured results of specific enthalpy, specific electrical resistivity and density of Ni80Cr20 are presented as a function of temperature as well as the derived quantities heat capacity, heat of fusion, thermal diffusivity and thermal conductivity. The composition of Ni80Cr20 is between pure nickel and highly alloyed materials. Therefore, its properties are compared to pure nickel and to Inconel 718 which has more than ten constituents and approximately 53% nickel and 18% chromium. Resistivity results show not only the intermediate position of the Ni80Cr20 alloy but also that an alloy can be quite different from the average of its constituents.

1. Introduction

The Subsecond Thermophysics Workgroup at TU Graz performed extensive research on pure metals. Currently this experience is extended to alloys. Industrial relevant alloys, such as Inconel 718, are designed by trial and error; the development requires a multitude of know-how in materials science. Therefore it is difficult to establish a relation between the ingredients of a composition and the effective properties. This investigation was performed on the alloy Ni80Cr20[1] (Ni78Cr22 at%) for the following reason: the correlation between a high-alloyed material (Inconel 718), its main pure element (Ni) and a simple alloy with a similar composition of the main constituents (Ni80Cr20) can be studied.

The investigation presented in this work deals mainly with high temperature properties, especially in the liquid state. However, most industrial relevant alloys are designed to meet mechanical properties in the solid state. Consequently, the well-known influence of add-ons in small quantities (e.g. rhodium, rhenium, molybdenum) on these mechanical properties (e.g. ductility) cannot be observed by this investigation technique. Finally, thermal treatments, such as quench hardening, lead to differing qualities, but cannot be quantified.

Nevertheless, small doses of alloying agents, or even impurities, can have a strong influence on the electrical resistivity in the solid state and some influence in the liquid state as well and since this quantity is a dominant parameter in some industrial processes and simulations [1], the present work is intended to provide data not only for basic research but also for the metal working industry.

Ni80Cr20 was chosen for measurement because it bridges the gap between pure nickel and Inconel 718, which consists of about 53% nickel and 18% chromium [2]. Both were studied repeatedly [3,4] and a revision of the measurements performed at TU Graz will be published [5].

2. Experimental

A typical analysis of Ni80Cr20 yields: Al 1000 ppm, Cr 18–20%, Fe 2000 ppm, Mn 2000 ppm, Si 1.5%, rest: Ni + Co [6]. Investigations were made on wire-shaped specimens (diameter nominal 0.5 mm) purchased from Advent Research Materials Ltd. Commercial names of this alloy are Nichrome® and Tophet®. It is used for electric resistance heating elements. The amount of 1.5% Si makes it a ternary alloy. Therefore, the use of a binary Ni-Cr phase diagram is not applicable to obtain solidus and liquidus temperatures. DTA measurements (STA 409 Netzsch, Selb, Germany), used for the following calculations, delivered solidus temperature T_s: 1661 K and liquidus temperature T_l: 1676 K ± 7 K. For the data evaluation, a density at room temperature of 8400 kg m^{-3} was used [7].

* Corresponding author. Tel.: +43 3168738649; fax: +43 3168738655.
E-mail addresses: thomas.huepf@tugraz.at (T. Hüpf), pottlacher@tugraz.at (G. Pottlacher).

[1] The name Ni80Cr20 is used throughout this paper regardless of the fact that the alloy contains 1.5% Si.

0040-6031/$ – see front matter © 2009 Elsevier B.V. All rights reserved.
doi:10.1016/j.tca.2009.04.015

When using this fast pulse-heating technique, wire shaped specimens are clamped in the center of a discharge chamber. During the experiment, a current pulse of about 10^5 A is conducted through the sample for several μs. Due to its ohmic resistivity, it heats rapidly (about 10^8 K/s). This high heating rate is the crucial point of this technique. It provides mechanical stability of the sample, even after the melting transition. The liquid sample with cylindrical geometry keeps its shape while it continues heating. At the boiling point the drastic volume increase leads to the so called 'wire explosion'. In summary this technique provides containerless handling of liquid metals and the short experimental duration (typically 50 μs) prevents chemical reactions.

The apparatus at TU Graz allows for several simultaneous measurements: Temperature is recorded by means of pyrometry under the assumption of a constant emissivity throughout the liquid phase (see [8] for more details on the legitimacy of this assumption). The surface radiation of the samples was detected with a pyrometer working at 1570 nm (FWHM 84 nm). The melting transition with its characteristic plateau in the voltage output of the pyrometer was used as calibration point (1676 K, end of melting). The two phase region of Ni80Cr20 is very narrow. This leads to a flat melting plateau. The current through the sample is recorded with an induction coil and real-time integration (Pearson-probe). Two knife-edge contacts, directly placed on the wire, provide the voltage drop. A fast CCD camera system is used to measure the volume expansion and the change of the sample geometry. To monitor the expanding diameter of the wire, it was backlit with a photoflash and a magnified picture was imaged by a specially designed CCD camera [9], which delivers a shadowgraph picture of a small portion of the wire each 5 μs. The diameter at room temperature is measured prior to the experiment with a digital laser-micrometer (Keyence, LS-7010) and the CCD profiles can be calibrated on the basis of this measurement.

By modifying experimental parameters it is possible to get pictures at different selected temperatures. These parameters are on the one hand the charging voltage of the capacitor bank (which acts as energy storage for the discharge current)—a slight increase leads to a higher heating rate and consequently the temperature is higher at the moment the CCD pictures are taken. On the other hand the framing sequence of the CCD camera can be shifted relatively to the heating process in steps of one microsecond. Thus an expansion picture can be 'directed' to every selected temperature.

From temperature dependent current, voltage and sample geometry, thermophysical properties such as enthalpy, electrical resistivity, density, thermal conductivity and thermal diffusivity as a function of temperature are calculated following the equations in Chapter 3. A detailed description of the experimental setup is given in [10].

The PC for data recording is placed inside a shielded room because the rapid alteration of electrical current can lead to disturbing electromagnetic fields. Each cable is run inside a copper pipe connected to this faraday-room. Sensitive electronics are placed in boxes of aluminum. Where necessary, TTL signals are converted to optical signals conducted in fiber optics to prevent electrical contact.

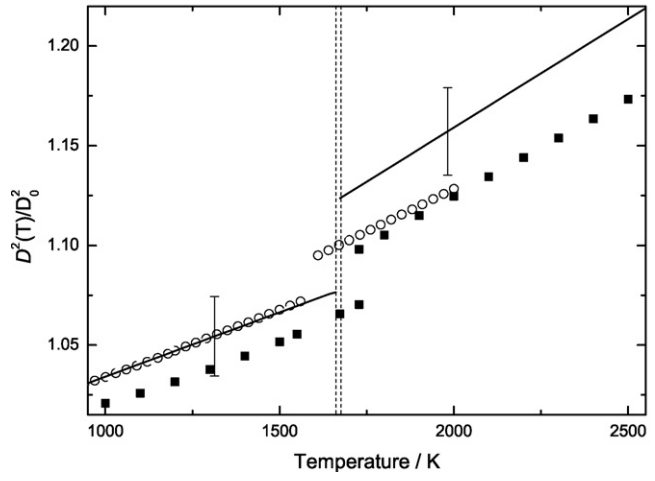

Fig. 1. Volume expansion ($D^2(T)/D_0^2$) of Ni80Cr20, nickel and Inconel 718 as a function of temperature. Solid lines: Ni80Cr20, filled squares: results for nickel [3], open circles: Inconel 718 [5], vertical dashed lines: solidus 1661 K and liquidus 1676 K.

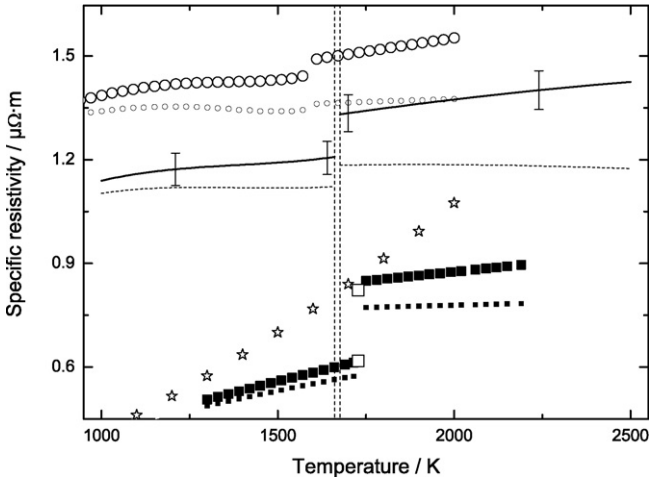

Fig. 2. Specific electrical resistivity of Ni80Cr20, nickel and Inconel 718 as a function of temperature. Solid lines: Ni80Cr20 including thermal expansion, dashed lines: Ni80Cr20 with initial geometry, filled squares: nickel [3] (big: including thermal expansion, small: without thermal expansion), open circles: Inconel 718 [5] (big: including thermal expansion, small: without thermal expansion), open stars: extrapolation of literature values of [11] for pure chromium, open rectangle: recommended value of [12] for Ni at T_m, vertical dashed lines: solidus 1661 K and liquidus 1676 K.

3. Results

3.1. Volume expansion

Fig. 1 presents the results of volume expansion obtained from ten independent measurements. The results in the vicinity of melting are excluded from the fits. In order to correspond to the cross section of the wire, the squares of the diameters are used.

The linear least squares fit for the solid phase is

$$D^2(T)/D_0^2 = 0.969 + 6.474 \times 10^{-5} T \quad 1000\,\mathrm{K} < T < 1661\,\mathrm{K} \tag{1}$$

and for the liquid phase

$$D^2(T)/D_0^2 = 0.941 + 1.091 \times 10^{-4} T \quad 1676\,\mathrm{K} < T < 2600\,\mathrm{K} \tag{2}$$

with D_0 being the diameter at room temperature.

3.2. Resistivity

Specific electrical resistivity of Ni80Cr20 as a function of temperature is shown in Fig. 2, together with the results for pure nickel [3] and Inconel 718 [5] (to maintain clearness of the plots, points are displayed regardless of the fact that the cited papers report polynomials). Resistivity with initial geometry ρ_{IG} (without considering thermal expansion) was calculated by the equation

$$\rho_{IG}(T) = \frac{U(T) \cdot \pi \cdot r^2}{I(T) \cdot l} \tag{3}$$

with U: voltage drop, I: current, r: radius at room temperature, l: length.

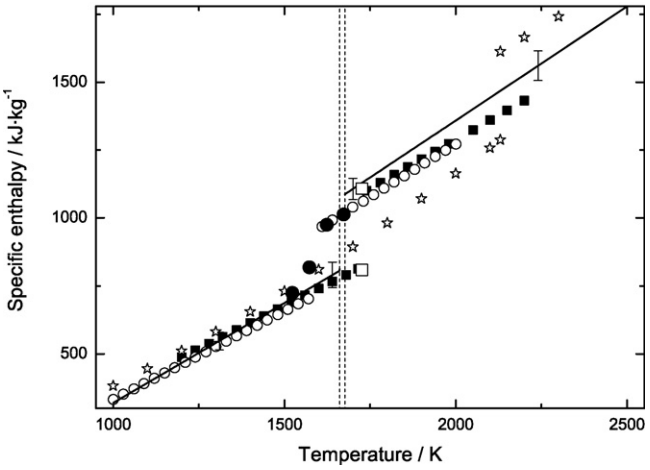

Fig. 3. Specific enthalpy of Ni80Cr20, nickel and Inconel 718 as a function of temperature. Solid lines: Ni80Cr20, filled squares: nickel [3], open circles: Inconel 718 [5], open rectangles: literature values of [13] for Ni, open stars: estimated value of [14] for Cr, full circles: literature values of [15] for Inconel 718, vertical dashed lines: solidus 1661 K and liquidus 1676 K.

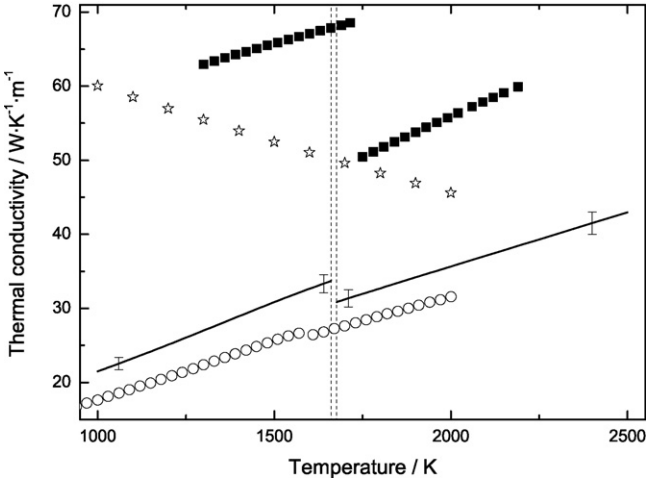

Fig. 4. Thermal conductivity of Ni80Cr20, nickel and Inconel 718 as a function of temperature. Solid lines: Ni80Cr20, filled squares: nickel (converted from [3]), open circles: Inconel 718 [5], open stars: literature values converted from [11], vertical dashed lines: solidus 1661 K and liquidus 1676 K.

The polynomial least squares fits for ρ_{IG} are (in μΩm)

$$\rho_{IG}(T) = 0.121 + 2.186 \times 10^{-3}T - 1.585 \times 10^{-6}T^2 + 3.806 \times 10^{-10}T^3 \quad 1100\,K < T < 1661\,K \tag{4}$$

for the solid phase and

$$\rho_{IG}(T) = 1.071 + 1.210 \times 10^{-4}T - 3.190 \times 10^{-8}T^2 \quad 1676\,K < T < 2500\,K \tag{5}$$

for the liquid phase. During the melting transition $\rho_{IG}(T)$ changes from 1.123 μΩm to 1.184 μΩm, which yields a resistivity change $\Delta\rho$ of 0.061 μΩm.

To account for volume expansion, changing the actual sample diameter, the resistivity with initial geometry $\rho_{IG}(T)$ has to be multiplied by $(D^2(T)/D_0^2)$ to obtain $\rho(T)$. The least squares fits are

$$\rho(T) = 0.022 + 0.240 \times 10^{-2}T - 1.689 \times 10^{-6}T^2 + 4.055 \times 10^{-10}T^3 \quad 1100\,K < T < 1661\,K \tag{6}$$

for the solid phase and

$$\rho(T) = 0.980 + 2.725 \times 10^{-4}T - 3.777 \times 10^{-8}T^2 \quad 1676\,K < T < 2500\,K \tag{7}$$

for the liquid phase. During the melting transition $\rho(T)$ changes from 1.207 μΩm to 1.331 μΩm, which yields a resistivity change $\Delta\rho$ of 0.124 μΩm.

3.3. Enthalpy and isobaric heat capacity

Specific enthalpy H was calculated from the electrical signals current and voltage drop by the equation:

$$H(t) - H(293\,K) = \frac{1}{m}\int I(t)\cdot U(t)dt \tag{8}$$

Herein m represents the mass of the sample obtained from the geometry and the density at RT (8400 kg m^{-3} [7]).

Results of specific enthalpy, $H - H_{RT}$ (starting at room temperature RT), as a function of temperature are shown in Fig. 3. Linear fits representing the measurement results are (in kJ kg^{-1})

$$H(T) = -417.3 + 0.737T \quad 1100\,K < T < 1661\,K \tag{9}$$

for the solid and

$$H(T) = -321.2 + 0.840T \quad 1676\,K < T < 2500\,K \tag{10}$$

for the liquid state, respectively. At the melting transition $H(T_s) = 807$ kJ kg^{-1} and $H(T_l) = 1087$ kJ kg^{-1}; thus a heat of fusion of $\Delta H = 280$ kJ kg^{-1} is obtained.

From its definition as the temperature derivative of enthalpy (under constant pressure), isobaric heat capacity c_p can be obtained from the slope of the linear enthalpy fits. The value for heat capacity in the solid state $c_{p,s}$ should only be regarded as a rough estimate and is limited to a narrow temperature range before the onset of melting, $c_{p,s} = 737$ J kg^{-1} K^{-1}. For the liquid phase $c_{p,l} = 840$ J kg^{-1} K^{-1} is obtained.

3.4. Thermal conductivity and thermal diffusivity

Thermal conductivity λ is calculated using the Wiedemann–Franz law.

$$\lambda(T) = \frac{L\cdot T}{\rho(T)} \tag{11}$$

The theoretical Lorenz-number L of 2.45×10^{-8} V^2 K^{-2} was taken as a first approach, although it may vary for different materials [16].

Results of thermal conductivity λ as a function of temperature are shown in Fig. 4. The linear fits (in W K^{-1} m^{-1}) are given by

$$\lambda(T) = 2.579 + 0.019T \quad 1100\,K < T < 1661\,K \tag{12}$$

for the solid, and by

$$\lambda(T) = 6.177 + 0.015T \quad 1676\,K < T < 2500\,K \tag{13}$$

for the liquid state. Thermal diffusivity a (in 10^{-5} m^2/s), calculated from

$$a(T) = \frac{L\cdot T}{\rho_{IG}\cdot c_p\cdot d} \tag{14}$$

with d: density at RT, is given by

$$a(T) = 1.573 \times 10^{-3} + 3.525 \times 10^{-4}T \quad 1100\,K < T < 1661\,K \tag{15}$$

$$a(T) = -5.178 \times 10^{-3} + 2.958 \times 10^{-4}T \quad 1676\,K < T < 2500\,K \tag{16}$$

More details on the calculations, the actual value of the Lorenz-number and a discussion of its influence on the uncertainty budget are given in [10].

4. Discussion

The phase diagram for Ni80Cr20 shows no phase transition in the solid state. The two phase region is very narrow (1661–1676 K) and subsequently the measured temperature traces show a flat melting plateau. The solidus–liquidus temperatures of the alloy are lower than the melting temperatures of its pure elements. DTA measurements yielded the transition temperatures of the material, which are slightly lower than the temperatures in the phase diagram of the binary Ni80Cr20 that may be expected due to the amount of 1.5% Si.

No measurements can be performed on pure chromium with our technique, because it is too brittle to be drawn as a wire. Therefore, the results for Ni80Cr20 are compared to the respective results for pure nickel and Inconel 718 which are described in detail in [3] and [5]. Although this work is based on a comparison inside a goal-oriented selection of materials measured under the same experimental conditions, the numerical values are of course to be compared with different techniques – that is to say literature values – as well. Thus we have added some to the graphs. A detailed comparison of nickel measurements was performed in [3], for Inconel 718 see [4] and [5].

The volume expansion (Fig. 1) of Ni80Cr20 is somewhat higher than the one of pure nickel. In the solid state Ni80Cr20 almost coincides with Inconel 718, but in the liquid state it is higher. The differences are very small and are not significant.

The electrical resistivity values are depicted in Fig. 2. Nickel has the lowest resistivity values, Inconel 718 the highest. The traces of each material are very similar, but differ in their absolute value. At 1676 K Inconel 718 has a resistivity of 1.502 μΩm, Ni80Cr20 has 1.331 μΩm, nickel: 0.604 μΩm and chromium approximately 0.750 μΩm. Ni80Cr20 is closer to the highly alloyed material Inconel 718 than to pure nickel in respect of resistivity. Additionally some datapoints of Zinovĭyev [11] (average data) for pure chromium are displayed to demonstrate, that the mixture of nickel and chromium does in no way lead to an average or weighted resistivity, but delivers much higher resistivity values. As expected, the (solid) solution has a higher electrical and thermal conductivity. The nickel values at melting agree very well with literature values of [12].

Fig. 3 depicts the results for enthalpy. Ni80Cr20 exhibits a slightly higher increase with increasing temperature than nickel and Inconel 718 and subsequently its heat capacity is higher too. The heat capacities in the liquid state are: Inconel 718: 778 J kg^{-1} K^{-1}, Ni80Cr20: 840.0 J kg^{-1} K^{-1}, nickel: 720.0 J kg^{-1} K^{-1}, chromium: 715.3 J kg^{-1} K^{-1} estimated value of [14]. Literature values for nickel [13] and Inconel 718 [15] at melting almost coincide with our respective measurements. The added literature values for chromium [14] clearly display, that the melting point of chromium is by far the highest out of this material selection (this complicates the interpretation of Fig. 3 and Fig. 2). Enthalpy values of all considered metals are very similar.

As the trends of thermal conductivity and thermal diffusivity are very similar, Fig. 4 depicts thermal conductivity only. It is evident, that the traces calculated according to (11) contain the reciprocal of the electrical resistivity. The strong resistivity increase of chromium with increasing temperature leads to a reversal of the trend in thermal conductivity (decreasing with increasing temperature).

It can be seen in Figs. 2 and 3 that the electrical resistivity as a transport property is much more sensitive to changes in composition. Heat capacities can be assumed similar to the respective pure elements, whereas electrical resistivity undergoes drastic changes. In the case of resistivity and thermal conductivity, Ni80Cr20 falls in the gap between pure nickel and Inconel 718. In the case of volume expansion and enthalpy the differences are alternating and too small to be judged.

5. Uncertainty

During the calculation of uncertainties two approaches are commonly used: the GUM [17] method, which obtains uncertainty by considering the propagation of the respective uncertainty of each input parameter and the (traditional) statistic approach, which obtains uncertainty by looking at the distribution of results.

Depending on the experimental setup and data acquisition the experimentalist chooses in which way uncertainty is calculated. Two examples will show that there can be contradicting results (for more details see [18]): If all experimental points are on a straight line, the statistic standard-deviation for the linear regression will be zero although the measurement devices can be defective. On the other hand, if the input parameters are exact but the results show big scattering, the statistic standard-deviation is exceeding the uncertainty calculated according to GUM (which in this case is zero).

The measurements performed in this work are of type one (statistic standard-deviation would deliver implausible small uncertainties) as the reproducibility is high. Only the thermal expansion measurements lead to considerable scattering. The significance of its fits can be increased by increasing the number of experimental points. Thus the statistic approach is the better choice.

The uncertainty analysis according to GUM [17] yields the following relative uncertainties for the Ni80Cr20 results (coverage factor 2): temperature: T: 2.5% (possible changes of emissivity in the liquid state not considered); enthalpy H: 3.5%; specific heat capacity c_p: 8%; specific electrical resistivity (at initial geometry) ρ_{IG}: 2.6%; electrical resistivity (including expansion) ρ: 3.3%; thermal conductivity (excluding the influence of the Lorenz number) λ: 3.7%; thermal diffusivity a: 8.8%. An elaborate uncertainty analysis of the measurements with the pulse-heating equipment at TU Graz according to GUM is given in [19].

Volume expansion (D^2/D_0^2): standard-deviation σ: 0.011, expressed as relative uncertainty with coverage factor 2: 2% (number of points: 25); diameter at room temperature D_0: ±1 μm (0.2%);

6. Conclusion

Investigations of alloys like Ni80Cr20 are currently in the focus of interest as they bridge the gap between pure elements and highly alloyed materials. The results for Ni80Cr20 are presented in this work and are compared to pure nickel and Inconel 718 measured under the same experimental conditions. They reveal that different types of connections are possible: First, the behaviour of the alloy is different from the average of its main constituents (see electrical resistivity). Regarding the possible applications of this alloy as heating elements, a higher electrical resistivity is wanted. Second, electrical resistivity of Ni80Cr20 is between nickel and Inconel 718 (but closer to Inconel 718). Third, the differences in specific enthalpy (Fig. 3) and volume expansion (Fig. 1) are small.

Acknowledgment

The project *Electrical Resistivity Measurement of High Temperature Metallic Melts* is sponsored by the Austrian Space Applications Programme (ASAP) of the FFG, Sensengasse 1, 1090 Wien.

References

[1] E. Kaschnitz, G. Pottlacher, Thermophysikalische Eigenschaften von Gießwerkstoffen, Giessereipraxis 1 (2002) 23–28.
[2] E.A. Loria (Ed.), Superalloy 718—Metallurgy and Application, The Minerals, Metals & Materials Society, TMS, Warrendale, 1989.
[3] B. Wilthan, C. Cagran, G. Pottlacher, Int. J. Thermophys. 25 (5) (2004) 1519–1534.
[4] G. Pottlacher, H. Hosaeus, E. Kaschnitz, A. Seifter, Scand. J. Metall. 31 (2002) 161–168.

[5] C. Cagran, W. Hohenauer, G. Pottlacher, Inconel 718—A Collection of Thermophysical Data from Quasistatic- and Transient-Measurement Techniques, in press.
[6] http://www.advent-rm.com (2008).
[7] http://www.goodfellow.com (2008).
[8] C. Cagran, C. Brunner, A. Seifter, G. Pottlacher, High Temp.—High Press. 34 (2002) 669–679.
[9] K. Preis, Thermophysikalische Daten von Nimonic 80A in der festen und flüssigen Phase, Diploma Thesis, Graz University of Technology, 2006.
[10] C. Cagran, T. Hüpf, B. Wilthan, G. Pottlacher, High Temp.—High Press. 37 (2008) 205–219.
[11] V. Zinovyev, Metals at High Temperatures—Standard Handbook of Properties, Hemisphere Publishing Corporation, New York, 1990.
[12] Y.S. Touloukian (Ed.), Properties of Selected Ferrous Alloying Elements, CINDAS Data Series on Material Properties III-1, McGraw-Hill Book Company, New York, 1981.
[13] H. Geoffray, A. Ferrier, M. Olette, Compt. Rend. 256 (1963) 139–141; R. Hultgren, P.D. Desai, D.T. Hawkins, M. Gleiser, K.K. Kelley, D.D. Wagman (Eds.), Selected Values of the Thermodynamic Properties of the Elements, Metals Park, American Society for Metals, 1973.
[14] R. Hultgren, P.D. Desai, D.T. Hawkins, M. Gleiser, K.K. Kelley, D.D. Wagman, Selected Values of the Thermodynamic Properties of the Elements, Metals Park, American Society for Metals, 1973.
[15] C.M. Kenneth, Recommended values of thermophysical properties for selected commercial alloys, Woodhead Publishing Ltd and ASM International, Cambridge England, 2002.
[16] P.G. Klemens, R.K. Williams, Int. Met. Rev. 31 (5) (1986) 197–215.
[17] Leitfaden zur Angabe der Unsicherheit beim Messen, DIN Deutsches Institut für Normung, 1., Beuth Verlag, Berlin, 1995.
[18] M. Matus, Technisches Messen, Oldenbourg Verlag 72 (2005) 584–591.
[19] B. Wilthan, Verhalten des Emissionsgrades und thermophysikalische Daten von Legierungen bis in die flüssige Phase mit einer Unsicherheitsanalyse aller Messgrößen, PhD Thesis, Technische Universität Graz, Austria, 2005.